Paper 44

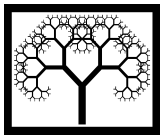

Proceedings of the Eighth International Conference on Engineering Computational Technology, B.H.V. Topping, (Editor), Civil-Comp Press, Stirlingshire, Scotland

An Isogeometric Approach for Free Vibration and Buckling Analysis of Laminated Composite Plates

N. Valizadeh[1], S. Shojaee[1], E. Izadpanah[1], T.Q. Bui[2] and V.T. Vu[3]
[1] Department of Civil Engineering, University of Kerman, Iran
[2] Department of Civil Engineering, University of Siegen, Germany
[3] School of Civil, Environmental and Architectural Engineering Korea University, Republic of Korea

Abstract

A NURBS-based isogeometric approach is developed for free vibration and buckling analyses of laminated composite plates using the classical plate theory (CPT). The NURBS basis function is employed for both the parameterization of the geometry and the approximation of plate deflection. The essential boundary conditions are presented through a weak form employing the Lagrange multiplier method and imposed using an orthogonal transformation technique. Several numerical examples for free vibration and buckling of laminated composite plates with various boundary conditions, fibre orientations and lay-up numbers are considered. The numerical results are compared with other existing solutions demonstrating the efficiency and high accuracy of the proposed approach for such problems.

Keywords: isogeometric analysis, NURBS, free vibration, buckling, laminated composite plates, Lagrange multiplier method.

1 Introduction

Due to the higher strength to weight and stiffness to weight ratios of composite materials compared with the conventional isotropic materials, laminated composites have been increasingly and widely used in a wide range of engineering structures and modern industries. Laminated composites also provide the convenient design through tailoring of the stacking sequence and layer thickness to optimize the desired characteristics for engineering applications. By a large requirement of using such laminated composite plates to engineering applications, studies involving the stability behaviours and natural vibrations of those structures are of great importance and essential in predicting their structural responses.
Isogeometric analysis is a novel computational approach which introduced by Hughes and co-workers in 2005 [1] with the aim of integrating the conventional

finite element method (FEM) and computer aided design (CAD). The method handles many great features shared by both the finite element method (FEM) and the meshless methods. The basic idea and also the heart of the IGA are to utilize the basis functions that are able to model accurately the exact geometries from the CAD points of view for numerical simulations of physical phenomena. It can be achieved by using the B-splines or Non Uniform Rational B-splines (NURBS) for the geometrical description and invoke the isoparametric concepts to define the unknown field variables, e.g. deflection in our case. A distinct advantage over the FEM is the mesh refinement is simply accomplished by re-indexing the parametric space without interaction with the CAD system. An intriguing trait of these functions is that they are typically smooth beyond the classical C^0-continuity of the standard FEM. The IGA-based approaches have constantly developed and shown many great advantages on solving many different problems in a wide range of research areas such as fluid-structure interaction, shells, structural analysis, and so on. Due to good inherent characteristics of the IGA method, developing an isogeometric finite element method associated with the NURBS shape functions for free vibration and buckling analysis of thin symmetrically laminated composite plates is presented in this research work. The present formulation is followed the classical plate theory (CPT). The finite element formulation based on the classical plate theory (Kirchhoff theory of plates) requires elements with at least C^1-inter-element continuity, which has gained many difficulties to achieve for the free-form geometries when using the standard Lagrangian polynomials as basis functions. As in the isogeometric analysis, higher order NURBS basis functions with an increased inter-element continuity can be easily obtained, the NURBS is well suited for the Kirchhoff elements. The approximation of the solution space for the deflection of the plate and the parameterization of the geometry are performed using NURBS-based approach. The essential boundary conditions are formulated separately from the discrete system equations by the aid of Lagrange multiplier method, while an orthogonal transformation technique is also applied to impose the essential boundary conditions in the discrete eigenvalue equation.

This paper is organized as follows: after the introduction, deriving the NURBS shape functions is presented immediately in the next section. In Section 3, governing equations and discretization are briefly introduced due to the sake of completeness. Comparative studies and numerical applications for the free vibration and buckling problems of laminated plates are presented in Section 4. Finally, concluding remarks are given in Section 5.

2 NURBS basis functions

Here, we present a brief review of some technical features of B-spline and NURBS basis functions for isogeometric analysis. For a detailed description of NURBS, readers are referred to [2].

Basically, a non-uniform rational B-spline (NURBS) curve $\mathbf{X}(\xi)$ of order p is defined as

$$\mathbf{X}(\xi) = \sum_{i=1}^{n} R_{i,p}(\xi)\tilde{\mathbf{X}}_i \tag{1}$$

$$R_{i,p}(\xi) = \frac{N_{i,p}(\xi)w_i}{\sum_{j=1}^{n} N_{j,p}(\xi)w_j} \tag{2}$$

where $R_{i,p}$ stands for the univariate NURBS basis functions, $\tilde{\mathbf{X}}_i = (x_i, y_i);\ i = 1, 2, ..., n$ are a set of n control points, w_i are a set of n weights corresponding to the control points that must be non-negative and $N_{i,p}$ represents the B-spline basis function of order p. To construct a set of n B-spline basis functions of order p, a knot vector Ξ is defined in a parametric space as follows:

$$\begin{aligned} &\Xi = \left\{\xi_1, \xi_2, ..., \xi_{n+p+1}\right\} \quad \xi_i \le \xi_{i+1}, \\ &i = 1, 2, ..., n+p \end{aligned} \tag{3}$$

The parametric space is assumed to be $\xi \in [0,1]$. The knot vector is said to be open if the knots are repeated $p+1$ times at the start and end of its vector. In this study, only open knot vectors are considered. Given a knot vector, the univariate B-spline basis function $N_{i,p}$ can be constructed by the following Cox-de Boor recursion formula [2]

$$N_{i,0}(\xi) = \begin{cases} 1 & \text{if } \xi_i \le \xi \le \xi_{i+1} \\ 0 & \text{otherwise} \end{cases} \tag{4}$$

and

$$N_{i,p}(\xi) = \frac{\xi - \xi_i}{\xi_{i+p} - \xi_i} N_{i,p-1}(\xi) + \frac{\xi_{i+p+1} - \xi}{\xi_{i+p+1} - \xi_{i+1}} N_{i+1,p-1}(\xi), \quad p = 1,\ 2,\ 3,\ \ldots\ . \tag{5}$$

The B-spline basis functions which are constructed from the open knot vectors have the interpolation feature at the ends of the parametric space. Figure 1 shows the quartic B-spline basis functions with the interpolation feature at the ends of the parametric space.

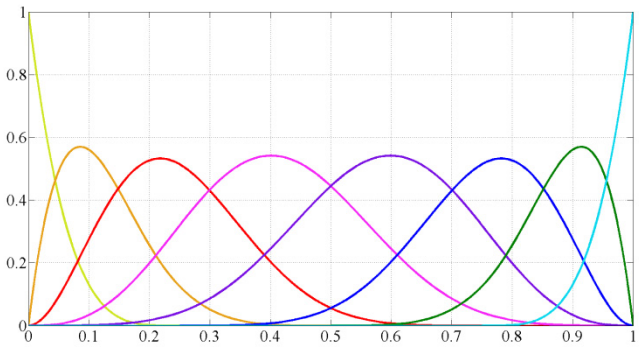

Figure 1: Quartic basis functions for an open knot vector
$\Xi = \{0,0,0,0,0,0.25,0.5,0.75,1,1,1,1,1\}$

Generally, a NURBS surface of order p in ξ direction and order q in η direction can be expressed as

$$\mathbf{X}(\xi,\eta) = \sum_{i=1}^{n}\sum_{j=1}^{m} R_{i,j}^{p,q}(\xi,\eta)\tilde{\mathbf{X}}_{i,j} = \sum_{i=1}^{n}\sum_{j=1}^{m} \frac{N_{i,p}(\xi)M_{j,q}(\eta)w_{i,j}}{\sum_{\hat{i}=1}^{n}\sum_{\hat{j}=1}^{m} N_{\hat{i},p}(\xi)M_{\hat{j},q}(\eta)w_{\hat{i},\hat{j}}}\tilde{\mathbf{X}}_{i,j} \qquad (6)$$
$$0 \le \xi,\eta \le 1$$

where $R_{i,j}^{p,q}$ stand for the bivariate NURBS basis functions, $\tilde{\mathbf{X}}_{i,j}$ is a control mesh of $n \times m$ control points, $w_{i,j}$ are the corresponding weights, while $N_{i,p}$ and $M_{j,q}$ are the B-spline basis functions defined on the Ξ and H knot vectors, respectively.

It is worthwhile to note that in isogeometric analysis, by using the isoparametric concept, the NURBS basis is employed for both the parameterization of the geometry and the approximation of the solution field, which is the plate deflection $w(\mathbf{x})$ in this paper, as follows:

$$w^h(\mathbf{x}(\boldsymbol{\xi})) = \sum_{I=1}^{n\times m} \phi_I(\boldsymbol{\xi}) w_I \qquad (7)$$

$$\mathbf{x}(\boldsymbol{\xi}) = \sum_{I=1}^{n\times m} \phi_I(\boldsymbol{\xi}) \tilde{\mathbf{x}}_I \qquad (8)$$

In all the above equations, $\boldsymbol{\xi} = (\xi,\eta)$ is the parametric coordinates, $\mathbf{x} = (x,y)$ is the physical coordinates, $\tilde{\mathbf{x}}_I$ represents the control points of a $n \times m$ control mesh, w_I represents the deflection of the plate at each control point, and $\phi_I(\boldsymbol{\xi})$ are the bivariate NURBS basis functions of order p and q in ξ and η directions, respectively.

3 Governing equations and discretization

3.1 Free vibration analysis

Consider a symmetrically laminated composite plate under Cartesian coordinate system with the thickness h in the $z-$direction and the fiber orientation θ of a layer, as depicted in Figure 2. The deflections of the plate in the (x, y, z) directions are denoted as (u, v, w), respectively. Based on the classical plate theory (CPT) [3], only the deflection of the plate $w(\mathbf{x})$ is chosen as the independent variable while the other two displacement components $u(\mathbf{x})$ and $v(\mathbf{x})$ can be obtained through $w(\mathbf{x})$. Therefore, the displacement fields of the Kirchhoff plate are obtained as,

$$\mathbf{u} = \{u \quad v \quad w\}^T = \left\{-z\frac{\partial}{\partial x} \quad -z\frac{\partial}{\partial y} \quad 1\right\}^T w = \mathbf{T}w \tag{9}$$

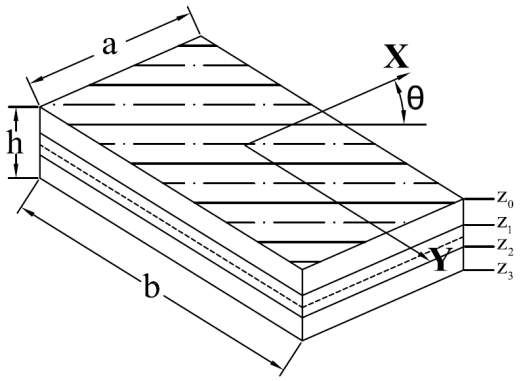

Figure 2: A schematic composite laminated plate

The pseudo-strains and pseudo-stresses of the plate are denoted as,

$$\boldsymbol{\varepsilon}_p = \left\{-\frac{\partial^2}{\partial x^2} \quad -\frac{\partial^2}{\partial y^2} \quad -2\frac{\partial^2}{\partial x \partial y}\right\}^T w = \mathbf{L}w \tag{10}$$

$$\boldsymbol{\sigma}_p = \{M_x \quad M_y \quad M_{xy}\}^T \tag{11}$$

where M_x, M_y and M_{xy} are bending and twisting moments, respectively. The pseudo-strains and pseudo-stresses are related in the form of the following generalized Hook's law for thin plates,

$$\boldsymbol{\sigma}_p = \mathbf{D}\boldsymbol{\varepsilon}_p \tag{12}$$

Due to the assumption of classical plate theory for a laminated composite plate, **D** can be written as,

$$\mathbf{D} = \begin{bmatrix} D_{11} & D_{12} & D_{16} \\ D_{12} & D_{22} & D_{26} \\ D_{16} & D_{26} & D_{66} \end{bmatrix} \tag{13}$$

$$D_{IJ} = \frac{1}{3}\sum_{k=1}^{N}(\bar{Q}_{IJ})_k(z_k^3 - z_{k-1}^3), \quad I,J = 1,2,6 \tag{14}$$

In the above equation, N is the number of layers of the composite laminated plate and $\bar{Q}_{IJ}$ is defined based on the material properties and the fiber orientation θ of each layer [3].

For free vibration analysis, the weak form of the elastodynamic undamped equilibrium equation of the plate can be expressed as,

$$\frac{d}{dt}\int_\Omega \rho \frac{\partial}{\partial \dot{w}}(\mathbf{T}\dot{w})^T(\mathbf{T}\dot{w})d\Omega + \int_\Omega \frac{\partial}{\partial w}(\mathbf{L}w)^T\mathbf{D}(\mathbf{L}w)d\Omega = 0 \tag{15}$$

In the above equation, the over-dot denotes the differentiation with respect to time. By substituting the deflection w from Equation (7) into Equation (15), and after some manipulations, the eigenvalue equations of the composite laminated plates can be obtained as,

$$(\mathbf{K} - \omega^2\mathbf{M})\bar{\mathbf{w}} = 0 \tag{16}$$

In this equation, ω indicates natural frequency, and $\bar{\mathbf{w}}$ is the eigenvector. **K** and **M**, respectively, stand for global stiffness and mass matrices which are defined as,

$$K_{IJ} = \int_\Omega \mathbf{B}_I^T\mathbf{D}\mathbf{B}_J d\Omega \tag{17}$$

$$M_{IJ} = \int_\Omega \left(I_m \frac{\partial \phi_I}{\partial x}\frac{\partial \phi_J}{\partial x} + I_m \frac{\partial \phi_I}{\partial y}\frac{\partial \phi_J}{\partial y} + \rho h \phi_I \phi_J \right) d\Omega \tag{18}$$

$$\mathbf{B}_I = \left\{ -\frac{\partial^2 \phi_I}{\partial x^2} \quad -\frac{\partial^2 \phi_I}{\partial y^2} \quad -2\frac{\partial^2 \phi_I}{\partial x \partial y} \right\}^T \tag{19}$$

in which $I_m = \rho h^3/12$ is the mass moment of inertia.

3.2 Buckling analysis

Consider a rectangular composite laminate subjected to in-plane forces

$\mathbf{N}=\left\{N_x, N_y, N_{xy}\right\}^T$ as depicted in Figure 3. The in-plane forces can be expressed as [3]

$$N_x=-N_0 \quad N_y=-\mu_1 N_0 \quad N_{xy}=-\mu_2 N_0 \tag{20}$$

where N_0 is a constant and μ_1 and μ_2 can be functions of coordinates.

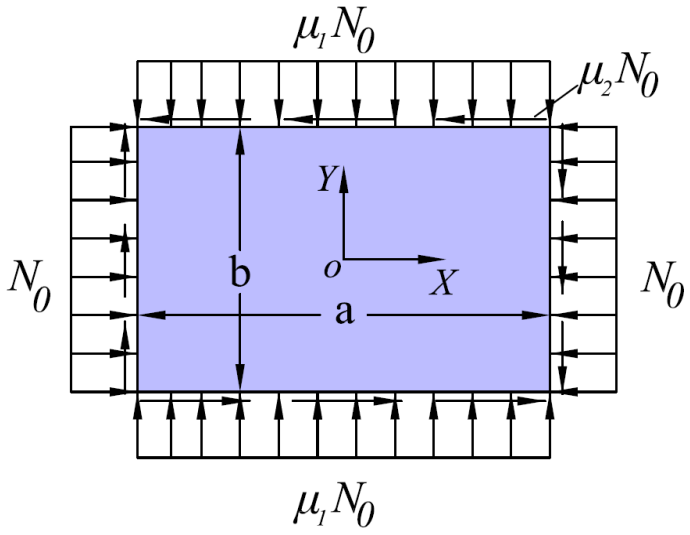

Figure 3: A rectangular plate subjected to in-plane forces

For buckling analysis, the weak form of equilibrium equation of the plate can be expressed as follows,

$$\int_\Omega \frac{\partial}{\partial w}(\mathbf{L}w)^T \mathbf{D}(\mathbf{L}w)d\Omega+\int_\Omega \frac{\partial}{\partial w}(\mathbf{L}w)^T \mathbf{N}d\Omega=0 \tag{21}$$

By substituting the deflection w from Equation (7) into the weak form defined as Equation (21), the final discrete equations for buckling analysis of the plate can be obtained as follows,

$$(\mathbf{K}-N_0\mathbf{G})\bar{\mathbf{w}}=0 \tag{22}$$

where $\mathbf{K}$ is the global stiffness matrix which has the same form as Eq. (17), and the matrix $\mathbf{G}$ is explicitly given by,

$$G_{IJ}=\int_\Omega\left[\frac{\partial\phi_I}{\partial x}\frac{\partial\phi_J}{\partial x}+\mu_1\frac{\partial\phi_I}{\partial y}\frac{\partial\phi_J}{\partial y}+\mu_2\left(\frac{\partial\phi_I}{\partial x}\frac{\partial\phi_J}{\partial y}+\frac{\partial\phi_J}{\partial x}\frac{\partial\phi_I}{\partial y}\right)\right]d\Omega \tag{23}$$

Solving this equation gives the static buckling values of the laminated composite plate which is subjected to in-plane loads.

3.3 Essential boundary conditions

Due to the non-interpolating nature of NURBS basis functions, the properties of Kronecker Delta are not satisfied. As a consequence, the essential boundary conditions need to be imposed by an appropriate approach. In this study, we merely adopt the Lagrange multiplier method [4,3] as its versatile means for treatment of such essential boundary conditions. In this way, the weak form of the essential boundary conditions associated with Lagrange multipliers is used to construct the discretized boundary conditions as follows:

$$\int_{\Gamma_u} \delta\lambda_d (w - \overline{w}) d\Gamma + \int_{\Gamma_u} \delta\lambda_r (r - \overline{r}) d\Gamma = 0 \tag{24}$$

where λ_d denotes the Lagrange multiplier related to the deflection, λ_r is the Lagrange multiplier associated with the rotation to the boundary, $\overline{w}$ represents the prescribed deflection, r is the rotation to the boundary while $\overline{r}$ being the prescribed rotation to the boundary.

Interpolating the Lagrange multipliers λ_d and λ_r using 1D Lagrange shape functions, the final discretized essential boundary equations can be written as,

$$\mathbf{H}_{2n_c \times n_{cp}} \mathbf{w}_{n_{cp} \times 1} = 0 \tag{25}$$

where n_c is the number of constraint points on the boundaries, $\mathbf{w} = \{w_1, w_2, ... \; w_{n_{cp}}\}^T$ represents the deflections at all the control points in the plate domain, and the matrix $\mathbf{H}$ is explicitly given by, respectively, for the simply supported boundaries

$$H_{KI} = \int_{\Gamma_u} \left[N_K^L \phi_I \quad N_K^L \phi_{I,nn} \right]^T d\Gamma \tag{26}$$

and for the clamped ones,

$$H_{KI} = \int_{\Gamma_u} \left[N_K^L \phi_I \quad N_K^L \phi_{I,n} \right]^T d\Gamma \tag{27}$$

where n is the unit normal to the boundary and N^L is the 1D Lagrange basis function. Since $\mathbf{H}$ is a singular matrix, the singular value decomposition [3] is used to decompose $\mathbf{H}$ as

$$\mathbf{H}_{2n_c \times n_{cp}} = \mathbf{U}_{2n_c \times 2n_c} \begin{bmatrix} \mathbf{S}_{r_k \times r_k} & 0 \\ 0 & 0 \end{bmatrix}_{2n_c \times n_{cp}} \mathbf{V}^T_{n_{cp} \times n_{cp}} \tag{28}$$

In Eq. (28), $\mathbf{U}$ and $\mathbf{V}$ are orthogonal matrices, $\mathbf{S}$ is a diagonal matrix which its elements are the singular values of the matrix $\mathbf{H}$, r_k denotes the rank of $\mathbf{H}$ which

equals to the number of independent constraints. Using the orthogonal transformation technique [3], $\mathbf{V}$ can be partitioned as

$$\mathbf{V}^T = \left\{ \mathbf{V}_{n_{cp} \times r_k} \quad \mathbf{V}_{n_{cp} \times (n_{cp} - r_k)} \right\}^T \tag{29}$$

Applying the coordinate transformation

$$\bar{\mathbf{w}} = \mathbf{V}_{n_{cp} \times (n_{cp} - r_k)} \tilde{\mathbf{w}} \tag{30}$$

Substituting the above equation in Equations (29) and (39), the eigenvalue equations for free vibration and buckling analysis in new coordinate system can be written as

$$(\tilde{\mathbf{K}} - \omega^2 \tilde{\mathbf{M}}) \tilde{\mathbf{w}} = 0 \tag{31}$$

$$\left(\tilde{\mathbf{K}} - N_0 \tilde{\mathbf{G}} \right) \tilde{\mathbf{w}} = 0 \tag{32}$$

where $\tilde{\mathbf{K}} = \mathbf{V}^T_{(n_{cp} - r_k) \times n_{cp}} \mathbf{K} \mathbf{V}_{n_{cp} \times (n_{cp} - r_k)}$. $\tilde{\mathbf{M}}$ and $\tilde{\mathbf{G}}$ can also be obtained in a similar fashion. It should be noted that these matrices are positive definite matrices which their dimensions are reduced using the orthogonal transformation technique.

4 Numerical examples

In this section, the validity and the accuracy of the proposed approach is demonstrated by free vibration and buckling analysis of different numerical examples with various boundary conditions. The results obtained by the proposed isogeometric analysis are also compared with other reference solutions available in the literature. For the convenience of comparisons, the normalized natural frequency parameter $\beta = \left(\dfrac{\omega^2 a^4 \rho h}{D_{0,1}} \right)^{1/2}$ with $D_{0,1} = E_1 h^3 / 12(1 - \nu_{12}\nu_{21})$ and the normalized buckling load factor $\beta = \dfrac{N_0 b^2}{\pi^2 D_{0,1}}$ are used.

Unless otherwise stated, the following material properties and geometrical parameters of square laminated plates are employed: ratio of elastic constants $E_1/E_2 = 2.45$ and $G_{12}/E_2 = 0.48$, Poisson's ratio $\nu_{12} = 0.23$, mass density $\rho = 8{,}000\,\mathrm{kg/m^3}$, length $a = b = 10\,\mathrm{m}$ and thickness $h = 0.06\,\mathrm{m}$.

4.1 Frequency and buckling analysis of symmetrically laminated square plates

The effect of the layer number and the boundary conditions of the composite laminates on the natural frequencies are investigated to demonstrate the validity of the present isogeometric code. For this purpose, the normalized natural frequencies of three- and five-ply square laminates with various orientations and different boundary conditions are examined and their results are then compared with the existing analytical and numerical solutions. For all calculations, cubic order NURBS basis function over an 11×11 control mesh is used. Tables 1 and 2 respectively, present the first six modes of the normalized frequencies for square three-ply laminate with fully simply supported (SSSS) and fully clamped (CCCC) boundary conditions.

Ply angle	Method	Mode					
		1	2	3	4	5	6
(0^o,0^o,0^o)	Present: IGA	15.17	33.25	44.39	60.69	64.54	90.20
	Chen et al. [6]	15.18	33.34	44.51	60.79	64.80	90.39
	Chow et al. [8]	15.19	33.31	44.52	60.78	64.55	90.31
	Leissa and Narita [9]	15.19	33.30	44.42	60.77	64.53	90.29
	Dai et al. [7]:CLPT	15.17	33.32	44.51	60.78	64.79	90.42
	Dai et al. [7]:TSDT	15.22	33.76	44.79	61.11	66.76	91.69
	Bui et al. [10]	15.06	33.30	44.36	59.52	65.95	89.53
	Exact [5]	15.17	33.25	44.39	60.68	64.46	90.15
(15^o,-15^o,15^o)	Present: IGA	15.42	34.08	43.87	60.86	66.70	91.54
	Chen et al. [6]	15.41	34.15	43.93	60.91	66.94	91.74
	Chow et al. [8]	15.37	34.03	43.93	60.80	66.56	91.40
	Leissa and Narita [9]	15.43	34.09	43.80	60.85	66.67	91.40
	Dai et al. [7]:CLPT	15.40	34.12	43.96	60.91	66.92	91.76
	Dai et al. [7]:TSDT	15.45	34.54	44.25	61.36	68.68	92.99
	Bui et al. [10]	15.39	34.56	44.23	61.32	66.91	91.40
(30^o,-30^o,30^o)	Present: IGA	15.93	35.90	42.67	61.62	71.84	85.91
	Chen et al. [6]	15.88	35.95	42.63	61.54	72.12	86.32
	Chow et al. [8]	15.86	35.77	42.48	61.27	71.41	85.67
	Leissa and Narita [9]	15.90	35.86	42.62	61.45	71.71	85.72
	Dai et al. [7]:CLPT	15.87	35.92	42.70	61.53	71.10	86.31
	Dai et al. [7]:TSDT	15.92	36.28	43.00	62.05	73.55	87.37
	Bui et al. [10]	15.86	36.05	42.70	61.33	71.48	86.01
(45^o,-45^o,45^o)	Present: IGA	16.19	37.00	41.90	62.09	77.26	80.17
	Chen et al. [6]	16.11	37.04	41.80	61.94	78.03	80.11
	Chow et al. [8]	16.08	36.83	41.67	61.65	76.76	79.74
	Leissa and Narita [9]	16.14	36.93	41.81	61.85	77.04	80.00
	Dai et al. [7]:CLPT	16.10	37.00	41.89	61.93	77.99	80.11
	Dai et al. [7]:TSDT	16.15	37.33	42.20	62.45	78.96	81.55
	Bui et al. [10]	16.01	37.05	41.68	61.40	78.20	81.12
(0^o,90^o,0^o)	Present: IGA	15.17	33.73	44.03	60.69	65.85	90.97
	Chen et al. [6]	15.18	33.82	44.14	60.79	66.12	91.16
	Bui et al. [10]	15.18	33.49	44.52	61.39	66.96	91.73

Table 1: The normalized natural frequencies of fully simply supported (SSSS) square three-ply laminated plate with various orientations

Ply angle	Method	Mode					
		1	2	3	4	5	6
$(0^o,0^o,0^o)$	Present: IGA	29.09	50.80	67.30	85.65	87.30	118.63
	Chen et al. [6]	29.27	51.21	67.94	86.25	87.97	119.3
	Chow et al. [8]	29.13	50.82	67.29	85.67	87.14	118.6
	Dai et al. [7]:CLPT	29.27	51.21	67.94	86.25	87.97	119.3
	Dai et al. [7]:TSDT	30.02	54.68	70.41	89.36	92.58	123.6
$(15^o,-15^o,15^o)$	Present: IGA	28.90	51.41	65.94	84.57	89.88	119.37
	Chen et al. [6]	29.07	51.82	66.54	85.17	90.56	120.0
	Chow et al. [8]	28.92	51.43	65.92	84.55	89.76	119.3
	Dai et al. [7]:CLPT	29.07	51.83	66.55	85.17	90.56	120.0
	Dai et al. [7]:TSDT	29.85	55.25	69.14	88.53	94.92	124.3
$(30^o,-30^o,30^o)$	Present: IGA	28.52	53.14	62.71	83.88	95.37	114.46
	Chen et al. [6]	28.69	53.57	63.24	84.43	96.13	115.4
	Chow et al. [8]	28.55	53.15	62.71	83.83	95.21	114.1
	Dai et al. [7]:CLPT	28.69	53.57	63.26	84.43	96.15	115.5
	Dai et al. [7]:TSDT	29.51	56.84	66.17	87.83	100.5	118.9
$(45^o,-45^o,45^o)$	Present: IGA	28.34	54.64	60.46	83.73	102.23	105.88
	Chen et al. [6]	28.50	55.11	60.91	84.25	103.2	106.7
	Chow et al. [8]	28.38	54.65	60.45	83.65	102.0	105.6
	Dai et al. [7]:CLPT	28.50	55.11	60.94	84.25	103.2	106.7
	Dai et al. [7]:TSDT	29.34	58.19	64.14	87.67	107.4	110.6
$(0^o,90^o,0^o)$	Present: IGA	29.09	51.51	66.77	85.65	89.06	119.63
	Chen et al. [6]	29.27	51.93	67.40	86.25	89.76	120.3

Table 2: The normalized natural frequencies of fully clamped (CCCC) square three-ply laminated plate with various orientations

Exact solutions [5] and the results obtained by other numerical approaches such as the EFG method by Chen et al. [6] and Dai et al. [7], the Rayleigh–Ritz method by Chow et al. [8], the Ritz method by Leissa and Narita [9] and the MKI method by Bui et al. [10] are also presented for comparison. The tabulated frequencies computed by the isogeometric analysis are perfectly approached to those of the compared studies. The natural frequencies for the five-ply laminates are compared in Table 3 with those obtained by Chow et al. [8], Bui et al. [10] and Leissa and Narita [9] showing an excellent agreement.

Next, the effect of different boundary conditions on the buckling load factor of a three-layer symmetrically laminated composite plate is investigated. The uniaxial in-plane compression load is applied in x-direction.

Table 4 presents the buckling load factors for this problem obtained by isogeometric analysis employing cubic NURBS basis function over an 11×11 control mesh. The results are also compared with those obtained by an exact solution [11] and also the EFG method [3,12]. Again, a very good agreement between the proposed approach and other methods is observed.

Boundary condition (Ply angle)	Method	Mode					
		1	2	3	4	5	6
SSSS:							
(15^o,-15^o,15^o,-15^o,15^o)	Present: IGA	15.49	34.27	43.92	61.59	66.50	91.62
	Chow et al. [8]	15.46	34.24	43.88	61.59	66.42	91.52
	Leissa and Narita [9]	15.50	34.30	43.93	61.62	66.48	91.51
	Bui et al. [10]	15.45	34.72	44.26	61.81	66.04	91.50
(30^o,-30^o,30^o,-30^o,30^o)	Present: IGA	16.11	36.64	42.63	63.51	71.65	85.99
	Chow et al. [8]	15.98	36.58	42.53	63.37	71.43	85.86
	Leissa and Narita [9]	16.10	36.64	42.62	63.45	71.60	85.88
	Bui et al. [10]	15.99	36.70	42.63	62.69	71.26	85.02
(45^o,-45^o,45^o,-45^o,45^o)	Present: IGA	16.42	38.38	41.43	64.51	78.04	79.30
	Chow et al. [8]	16.29	38.30	41.32	64.35	77.77	79.09
	Leissa and Narita [9]	16.40	38.37	41.40	64.41	77.94	79.23
	Bui et al. [10]	16.24	38.31	41.18	63.15	77.72	80.41
CCCC:							
(15^o,-15^o,15^o,-15^o,15^o)	Present: IGA	28.97	51.63	66.02	85.57	89.52	120.54
	Chow et al. [8]	29.00	51.65	66.01	85.55	89.40	120.5
(30^o,-30^o,30^o,-30^o,30^o)	Present: IGA	28.74	53.96	62.76	86.14	95.17	114.65
	Chow et al. [8]	28.78	53.98	62.76	86.09	95.04	114.4
(45^o,-45^o,45^o,-45^o,45^o)	Present: IGA	28.62	56.32	59.94	86.53	103.20	105.07
	Chow et al. [8]	28.68	56.34	59.94	86.48	103.0	104.9

Table 3: The normalized natural frequencies of fully simply supported (SSSS) and fully clamped (CCCC) square five-ply laminated plate with various orientations

Boundary condition (Ply angle)	Method	Boundary condition			
		SSSS	CCCC	CSCS	SCCS
(0^o,0^o,0^o)	Present: IGA	2.36	6.71	4.27	3.93
	EFG [3,12]	2.39	6.78	4.34	3.97
	Exact [11]	2.36	-	-	-
(10^o,-10^o,10^o)	Present: IGA	2.40	6.64	4.33	3.95
	EFG [3,12]	2.42	6.72	4.39	3.97
(15^o,-15^o,15^o)	Present: IGA	2.43	6.57	4.41	3.96
	EFG [3,12]	2.45	6.64	4.46	3.96
(20^o,-20^o,20^o)	Present: IGA	2.48	6.48	4.51	3.97
	EFG [3,12]	2.49	6.55	4.56	3.96
(30^o,-30^o,30^o)	Present: IGA	2.59	6.29	4.79	4.00
	EFG [3,12]	2.57	6.36	4.84	3.96
(40^o,-40^o,40^o)	Present: IGA	2.65	6.15	4.90	4.01
	EFG [3,12]	2.63	6.21	4.91	3.94
(45^o,-45^o,45^o)	Present: IGA	2.66	6.10	4.78	4.01
	EFG [3,12]	2.64	6.16	4.79	3.93
(0^o,90^o,0^o)	Present: IGA	2.36	6.70	4.36	3.93
	EFG [3,12]	2.39	6.78	4.43	3.97
	Exact [11]	2.36	-	-	-

Table 4: The uniaxial buckling load factor of square three-ply laminated plate with different boundary conditions and various orientations subjected to uniaxial compression

4.2 Frequency analysis of symmetrically laminated composite elliptical plates

In this example, the natural frequencies are calculated for elliptical laminates. The radii of the elliptical laminates are $a = 5m$ and $b = 2.5m$, respectively. Other geometrical and material parameters are set the same as square laminate. Cubic order NURBS basis function with 196 control points is used for discretization of the problem. In Figure 4, control points and physical mesh are shown. This problem has been investigated by Bui et al [10] for three- and five-ply composite plate with fully simply supported boundary condition, and by Chen et al. [6] for three-ply composite plate clamped at all edges. The normalized first nine frequencies of the three-ply laminated plate for the fully simply supported and fully clamped boundaries are presented in Tables 5 and 6 with various fiber orientations, respectively. The results are also compared with reference solutions [10,6] and an excellent agreement is again found as expected. In addition, the first eight mode shapes of fully clamped three-ply elliptical composite plate with $(45^o, -45^o, 45^o)$ are illustrated in Figure 5.

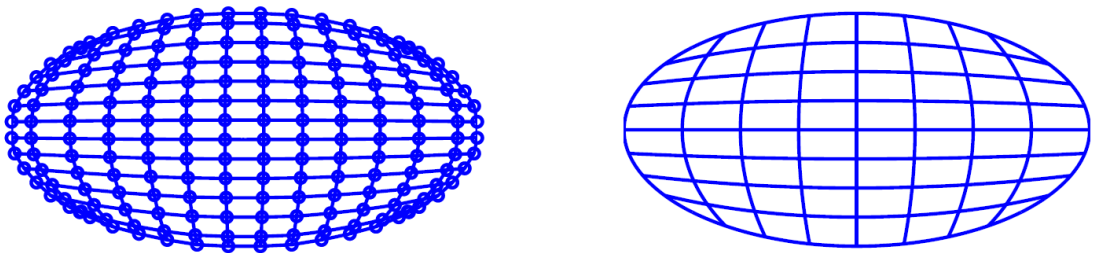

Figure 4: An elliptical plate with 196 control points and 64 elements (*left*) Control mesh (*right*) Physical mesh

Angle ply	Method	Mode								
		1	2	3	4	5	6	7	8	9
$(0^o,0^o,0^o)$	IGA	8.78	17.83	30.11	31.71	43.33	50.65	60.69	63.98	75.27
	MKI [10]	8.97	18.11	31.77	32.12	44.14	50.85	-	-	-
$(15^o,-15^o,15^o)$	IGA	8.96	18.03	30.79	31.40	44.64	49.40	62.28	65.35	72.52
	MKI [10]	9.12	18.26	31.92	32.30	44.92	49.90	-	-	-
$(30^o,-30^o,30^o)$	IGA	9.49	18.39	30.80	32.96	47.28	47.44	64.94	68.36	70.06
	MKI [10]	9.61	18.55	31.35	34.12	47.06	47.61	-	-	-
$(45^o,-45^o,45^o)$	IGA	10.34	18.66	30.08	36.43	45.23	50.42	64.71	67.09	77.92
	MKI [10]	10.41	18.76	30.57	37.36	45.04	49.96	-	-	-
$(0^o,90^o,0^o)$	IGA	8.95	17.89	30.78	31.62	43.92	50.38	61.18	65.46	74.83
	MKI [10]	9.14	18.16	32.03	32.45	44.73	50.56	-	-	-

Table 5: The normalized natural frequencies of fully simply supported (SSSS) elliptical three-ply laminate with various orientations

Angle ply	Method	Mode								
		1	2	3	4	5	6	7	8	9
$(0^o,0^o,0^o)$	IGA	18.44	29.16	44.81	45.57	60.01	65.35	78.81	85.83	91.31
	EFG [6]	18.48	29.38	44.97	45.72	60.44	65.33	79.24	85.31	91.50
$(15^o,-15^o,15^o)$	IGA	18.78	29.48	44.56	46.57	61.67	64.06	80.67	87.64	88.56
	EFG [6]	18.83	29.70	44.73	46.72	62.06	64.07	81.09	87.14	88.90
$(30^o,-30^o,30^o)$	IGA	19.85	30.22	44.16	49.81	61.88	65.45	84.04	84.16	93.88
	EFG [6]	19.89	30.44	44.34	49.95	61.94	65.77	84.63	84.81	93.36
$(45^o,-45^o,45^o)$	IGA	21.57	31.17	43.92	55.07	60.06	69.96	80.18	87.61	104.42
	EFG [6]	21.60	31.38	44.11	55.17	60.19	70.21	81.64	88.25	103.7
$(0^o,90^o,0^o)$	IGA	18.77	29.36	44.83	46.58	60.91	65.14	79.55	87.82	90.87
	EFG [6]	18.81	29.58	44.99	46.72	61.34	65.14	79.99	87.23	91.16

Table 6: The normalized natural frequencies of fully clamped (CCCC) elliptical three-ply laminate with various orientations

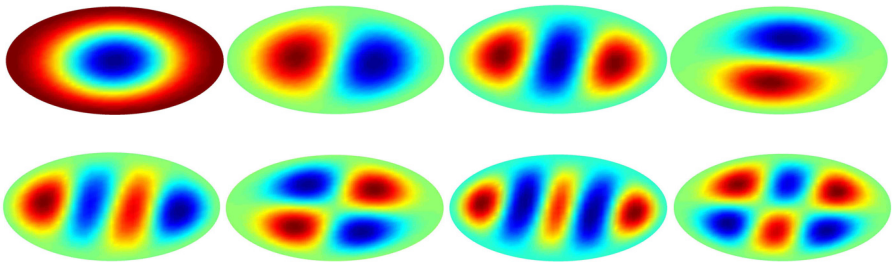

Figure 5: The first eight mode shapes of fully clamped three-ply elliptical composite plate with $(45^o,-45^o,45^o)$

Next, we study the computational efficiency (CPU-time) of the present IGA method for the free vibration analysis of a fully simply supported three-layer laminate arranged as $(0^o,0^o,0^o)$. For serving the comparison purpose, a solution based on the standard EFG method is also performed for this problem in such a way. The programs are compiled on a personal computer with Intel Core 2 CPU-2.40 GHz and 4GB of RAM. Three different densities of 121, 196 and 289 control points or nodes are considered. Basically, the estimation here is to measure the CPU-time spent in constructing the global stiffness matrix, imposing the essential boundary conditions and solving the algebraic equations. The fundamental frequency and the computational time for isogeometric analysis using quadratic and cubic NURBS and the EFG employing quadratic basis function are reported in Table 7. The computational time versus number of control points or nodes are also plotted in Figure 6. It can be observed from the results that the quadratic and cubic IGA are much more efficient than the quadratic EFG. Obviously, there may have different reasons that make the EFG method costs higher than the IGA significantly. The key point behind this result may lie in the fact that an expensive price of generating the meshless shape functions is often required. From the algorithm of the meshless method, it can also be seen that the meshless shape functions vary from quadrature point to point generated during the implementation process, which totally differs from the IGA whose basis functions are predefined before simulation.

Method	Number of control points/nodes	Fundamental frequency	Computational time (s)
IGA-Quadratic	121	8.866	2.353
IGA-Cubic		8.786	3.042
EFG		8.940	3.464
IGA-Quadratic	196	8.829	4.093
IGA-Cubic		8.781	5.486
EFG		8.924	6.862
IGA-Quadratic	289	8.812	6.588
IGA-Cubic		8.780	9.000
EFG		8.809	15.690

Table 7: Comparison of the computational time and the normalized fundamental frequency of fully simply supported (SSSS) elliptical three-ply laminate arranged as $(0^o, 0^o, 0^o)$ among IGA and EFG methods

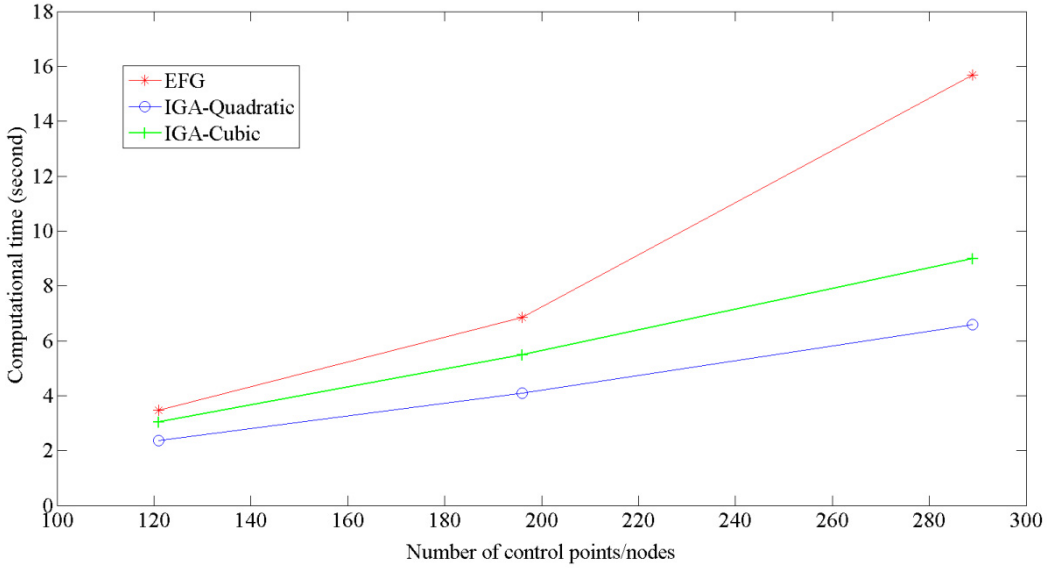

Figure 6: Comparison of the computational time between the IGA and the EFG

5 Conclusion

We have successfully presented an application of the NURBS-based isogeometric finite element approach to free vibration and buckling analysis of thin laminated composite plates. Several numerical examples with different boundary conditions have been considered and the achieved natural frequencies or critical buckling loads are investigated and validated with the ones derived from analytical and other existing numerical methods. The numerical results definitely show that the proposed approach can yield accurate solutions of the eigenvalue problems compared to other existing methods available in the literature. The computational efficiency has also analysed and the gained comparison shows very much efficiency to the IGA compared with the EFG. As a result many advantages of the IGA approach, *e.g.* in

modelling exact geometries with the aid of the NURBS method, high-order continuity, etc. the IGA has been developed rapidly for dealing with many engineering problems, in which problems in advanced multifiled materials, e.g. piezoelectric, magnetoelectroelastic, are appropriate.

References

[1] T.J.R. Hughes, J.A. Cottrell, Y. Bazilevs, "Isogeometric analysis: CAD, finite elements, NURBS, exact geometry and mesh refinement", Computer Methods in Applied Mechanics and Engineering, 194, 4135-4195, 2005.

[2] L. Piegl, W. Tiller, "The NURBS book (Monographs in Visual Communication)", Springer-Verlag, Second edition, New York, 1997.

[3] G.R. Liu, "Meshfree Methods: Moving Beyond the Finite Element Method", CRC Press, Boca Raton, 2003.

[4] T. Belytschko, Y.Y. Lu, L. Gu, "Element free Galerkin method", International Journal for Numerical Methods in Engineering, 37, 229-256, 1994.

[5] J.M. Whitney, "Structural analysis of laminated anisotropic plates", Technomic Publishing Company Inc, Pennsylvania, USA, 1987.

[6] X.L. Chen, G.R. Liu, S.P. Lim, "An element free Galerkin method for the free vibration analysis of composite laminates of complicated shape", Composite Structures, 59, 279-289, 2003.

[7] K.Y. Dai, G.R. Liu, M.K. Lim, X.L. Chen, "A mesh-free method for static and free vibration analysis of shear deformable laminated composite plates", Journal of Sound and Vibration, 269, 633-652, 2004.

[8] S.T. Chow, K.M. Liew, K.Y. Lam, "Transverse vibration of symmetrically laminated rectangular composite plates", Composite Structures, 20, 213-226, 1992.

[9] A.W. Leissa, Y. Narita, "Vibration studies for simply supported symmetrically laminated rectangular plates", Composite Structures, 12, 113-132, 1989.

[10] Q.T. Bui, N.M. Nguyen, Ch. Zhang, "An efficient meshfree method for vibration analysis of laminated composite plates", Computational Mechanics; 48, 175-193, 2011.

[11] Y. Narita, A.W. Leissa, "Buckling studies for simply supported symmetrically laminated rectangular plates", International Journal of Mechanical Sciences, 32, 909-924, 1990.

[12] G.R. Liu, X.L. Chen, J.N. Reddy, "Buckling of symmetrically laminated composite plates using the element-free Galerkin method", International Journal of Structural Stability and Dynamics, 2, 281-294, 2002.